Electrochemical and Solid-State Letters, **12** (2) A33-A38 (2009)
1099-0062/2008/12(2)/A33/6/$23.00 © The Electrochemical Society

Vanadium Modified $LiFePO_4$ Cathode for Li-Ion Batteries

Jian Hong,[a,*] C. S. Wang,[b,] X. Chen,[c,**] S. Upreti,[a] and M. Stanley Whittingham[a,***,z]**

[a]*Department of Chemistry and Materials Science, State University of New York at Binghamton, Binghamton, New York 13902-6000, USA*
[b]*Department of Chemical Engineering, University of Maryland, College Park, Maryland 20742, USA*
[c]*Department of Chemistry, University of Houston, Houston, Texas 77004, USA*

The structure and electrochemical behavior of vanadium-modified olivine $LiFePO_4$ was investigated. Vanadium was found to be incorporated into the olivine structure on the phosphorus site, not on the iron site, with the unit cell decreasing in size as the vanadium content increases. Material synthesized under reducing conditions with 5% vanadium gave materials with the best electrochemical performance. The rate capability of nanostructured $LiFeP_{0.95}V_{0.05}O_4$ was comparable to the best nanosized $LiFePO_4$ formed solvothermally while using less than 1/3 the amount of carbon conductor. The vanadium does not appear to be electrochemically active within the voltage cycling window of $LiFePO_4$.
 [DOI: 10.1149/1.3039795]

Manuscript submitted October 3, 2008; revised manuscript received November 6, 2008. Published December 8, 2008.

Olivines have been the subject of intensive study since the original work of Padhi et al.[1] showed they exhibited redox behavior. Complete solid solution on the iron site has been found for most divalent cations of comparable size,[2,3] and such behavior is found in nature, for example, in simferite, $LiMg_{0.5}Fe_{0.3}Mn_{0.2}PO_4$.[4] However, there has been much disagreement over whether aliovalent cation substitution can be accomplished, with Chung et al.[5] being a strong proponent of the benefits of aliovalent substitution, Herle et al.[6] suggesting that those benefits are due to the formation of a conductive film of Fe_2P, and Islam et al.[7] reporting theoretical studies indicating that aliovalent substitution is not possible.

If indeed a trivalent cation could be incorporated onto the iron site, then that might lead to vacancies on the lithium site because of the need for charge balance. Those vacancies might be expected to lead to an enhanced lithium-ion conductivity, and therefore higher power capabilities, a key requirement for batteries to be used for electric vehicle propulsion, whether in hybrid electric vehicles, plug-in hybrid electric vehicles, or all electric configurations. Olivine $LiFePO_4$ is one prime candidate for such use because of its low-cost-component features, high stability, and environmental friendliness. Low electronic conductivity has been overcome by coating the surface of the particles with conductive films of carbon or phosphide, or by grinding with carbon powder.[5,6,8,9] The reaction mechanism involves a phase front, between the two phases $LiFePO_4$ and $FePO_4$, moving through the material;[10] this phase front motion and rate capability might be enhanced by incorporating nonpinning defects into the structure that could reduce the nucleation energy for forming these two-phase boundary regions. This nucleation energy might also be reduced by going to nanosized material, which also leads to some single-phase behavior.[11-14] If the particles are sufficiently small it has been postulated[15] that the compound Li_xFePO_4 exists for all values of x from zero to unity. This could result in much faster kinetics, as one would have a homogeneous cathode, much as in Li_xTiS_2.[16] However, the tap density drops drastically as the particle size decreases and the carbon coating content increases,[17] so the use of nanosized materials might lead to high power but could result in very low volumetric energy storage.

Vanadium forms a number of electrochemically active phosphates, such as $VOPO_4$, which can readily react with one or more lithium atoms.[18] Both iron and vanadium form Nasicon structures, $Li_3M_2(PO_4)_3$, but there is no clear published evidence that vanadium can be incorporated into the olivine lattice. Wen et al.[19] showed an improved electrochemical activity of $LiFe_{0.9}V_{0.1}PO_4$ over pure $LiFePO_4$, but the latter had very poor electrochemical characteristics of only around 100 mAh/g; moreover, there was no structural evidence for vanadium substitution; the lattice parameters were the same. Yang et al.[20] showed that a two-phase mixture of the olivine $LiFePO_4$ and the Nasicon $Li_3V_2(PO_4)_3$ had enhanced electrochemical behavior over either single phase. The electrochemical behavior clearly shows the discharge plateaus of both phases, but again the electrochemical capacity of the pure $LiFePO_4$ was poor. We therefore decided to determine whether indeed vanadium can be incorporated into the olivine structure, and whether its presence results in enhanced electrochemical behavior in micrometer-size material. We attempted to form the $LiFe_{1-y}V_yPO_4$ solid solution for $0 \leqslant y \leqslant 0.2$ under nonoxidizing and reducing conditions, but formed $LiFeP_{1-y}V_yO_4$, and report here their structural properties and electrochemical behavior. The electrochemical behavior is compared to that of the nanosized $LiFePO_4$[11,12] materials.

Experimental

Synthesis.— Lithium carbonate (Sigma-Aldrich, >99%), iron(II) oxalate tetra-hydrate (Sigma-Aldrich, >99%), ammonium phosphate (Sigma-Aldrich, >99%), and NH_4VO_3 (Sigma-Aldrich, >99%) were used as the precursors. The stoichiometric precursors (with the composition of $LiFePO_4$, $LiV_{0.05}Fe_{0.95}PO_4$, $LiV_{0.075}Fe_{0.925}PO_4$, $LiV_{0.1}Fe_{0.9}PO_4$, $LiV_{0.15}Fe_{0.85}PO_4$, and $LiV_{0.2}Fe_{0.8}PO_4$) were ballmilled in acetone for 4 days and then dried, ground, and sieved with 200 mesh sieve before firing in one of four gases (nitrogen, argon, nitrogen with 5% H_2, and argon with 5% H_2). The ground precursors were first decomposed at 350°C for 3 h to drive out the gases and then the temperature was raised to 700°C. After keeping the temperature at 700°C for 6 h, the materials were cooled to room temperature with a rate of 10°C/min.

Characterization.— The microstructure was determined using high-resolution scanning electron microscopy (SEM), FEI Quanta 200 with an energy-dispersive spectrometer. The $LiFePO_4$ powder was attached directly to a carbon tape and then coated with a 10 Å layer of gold. Powder X-ray diffraction (XRD) was performed on a Rigaku ARC5 diffractometer with Cu Kα radiation.

Electrochemical measurements.— The electrodes consisted of 88% $LiFePO_4$ powder, 6% carbon black, and 6% polyvinylidene fluoride (Kynar, Elf-Atochem) in 1-methyl-2-pyrrolidinone solvent. A slurry of the mixture was coated onto an Al foil current collector to form a disk electrode of area of 1.2 cm^2 containing ca. 6 mg of active $LiFePO_4$ for coin cells and a square electrode with an area of 6 cm^2 containing ca. 24 mg of active $LiFePO_4$ for pouch cells. After drying in an oven at 120°C overnight, the electrodes were pressed at 1 ton/cm^2 for 10 min. Both the pouch cells and coin cells were set up in an argon-filled glove box. In the pouch cells the positive and

* Electrochemical Society Student Member.
** Electrochemical Society Active Member.
*** Electrochemical Society Fellow.
z E-mail: stanwhit@gmail.com

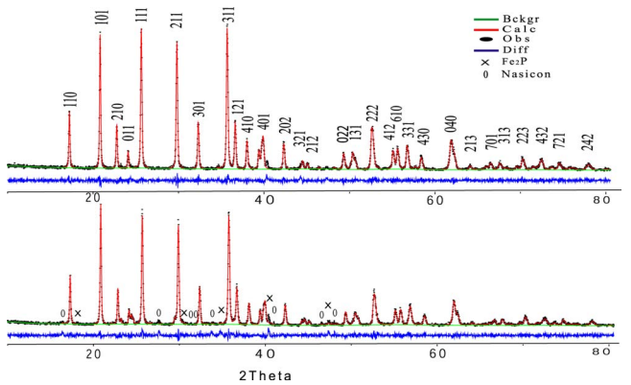

Figure 1. (Color online) XRD patterns of (top) 5% and (bottom) 15% vanadium-substituted $LiFePO_4$ formed in 5% H_2 in argon atmosphere. The top figure shows the Miller indexes and the bottom one the two impurity phases, Fe_2P and Nasicon, $Li_3Fe_2(PO_4)_3$. The Rietveld difference plots are shown below each diffraction pattern.

negative electrodes were separately laminated to their respective current collector grids on one side and a polymer separator on the other side. The two plastic films were laminated with the reference electrode in the middle. The coin cells were made with a coin cell machine (Hohsen Corp., Japan). Galvanostatic charge and discharge was performed with an Arbin cycler at current densities corresponding to 0.1, 0.5, 1, 5, and 10 C rates in the coin cell. Lithium metal was used as both counter and reference electrode, $LiPF_6$ in ethylene carbonate/propylene carbonate/dimethyl carbonate/ethyl methyl carbonate (1:1:1:3 by volume) was used as the electrolyte, and the cathodes were cycled between 2.0 and 4.2 V vs lithium metal, unless specified. Electrochemical impedance studies used a Solartron electrochemical interface (1287) and frequency analyzer (1260) using a three-electrode pouch cell in the frequency range of 500 Khz to 20 mHz. The galvanostatic intermittent titration (GITT) was tested in a coin cell with a current of less than 20 $\mu A/cm^2$.

Table I. Lattice parameters for the $LiFeP_{1-y}V_yO_4$ phases.

Vanadium, y	a (Å)	b (Å)	c (Å)	Volume (Å^3)
$LiFePO_4$	10.3267(3)	6.0064(2)	4.6945(1)	291.19(2)
0.05	10.3159(4)	6.0016(2)	4.6945(2)	290.64(2)
0.15	10.3028(6)	5.9953(4)	4.7007(3)	290.35(5)
Ref. 21	10.264	5.996	4.683	288.22

Results and Discussion

Phase characterization.— Samples were prepared in hydrogen-free and 5% hydrogen atmospheres. The hydrogen prevents the formation of ferric species and might help reduce the oxidation state of the vanadium precursor but can lead to the formation of Fe_2P.[6] The last, if present, could provide an electronically conducting surface that could help the electrochemical properties. The powder XRD patterns of all the materials formed could be indexed to the orthorhombic crystal structure (space group *pmnb*) of triphylite, with no impurities being detected in the vanadium-absent or low-vanadium samples. However, the XRD patterns of the higher vanadium content compounds do show an indication of impurities $Li_3V_2(PO_4)_3$, Li_3PO_4, or Fe_2P phases. Figure 1 shows the XRD patterns for the 5

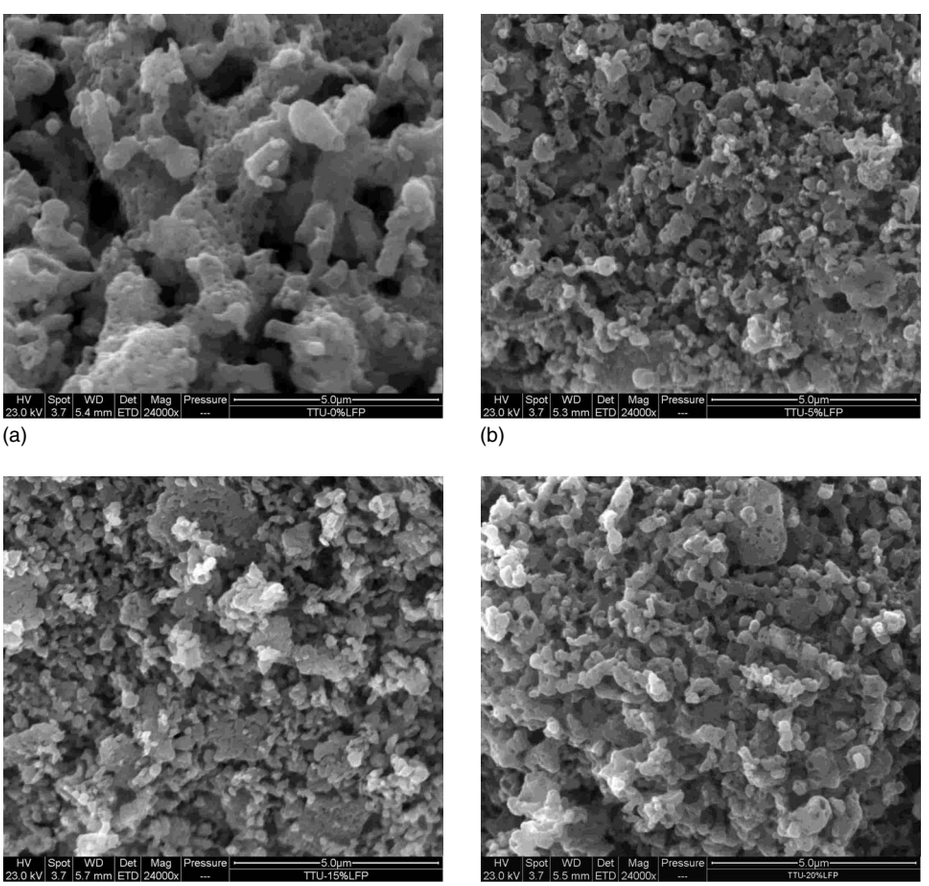

Figure 2. SEM of the $LiFeP_{1-y}V_yO_4$ material after heat-treatment in 5% hydrogen in argon, (a) $y = 0$, (b) $y = 0.05$, (c) $y = 0.15$, and (d) $y = 0.2$. Each frame is about 10×10 μm in size. (The features discussed in the text are best seen by enlarging the figures on a computer screen.)

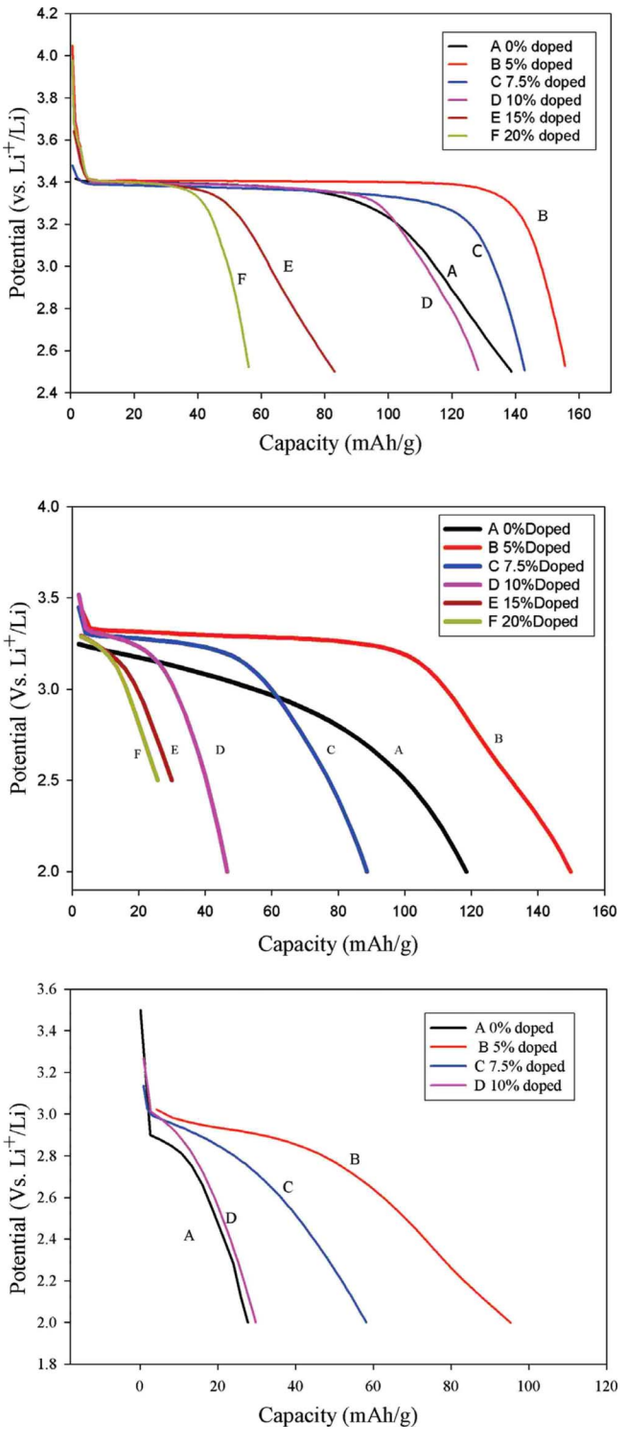

Figure 3. (Color online) The electrochemical capacity of $LiFeP_{1-y}V_yO_4$ heat-treated in 5% hydrogen in argon at (top) 0.1 C, (bottom) C, and (bottom) 10 C rates.

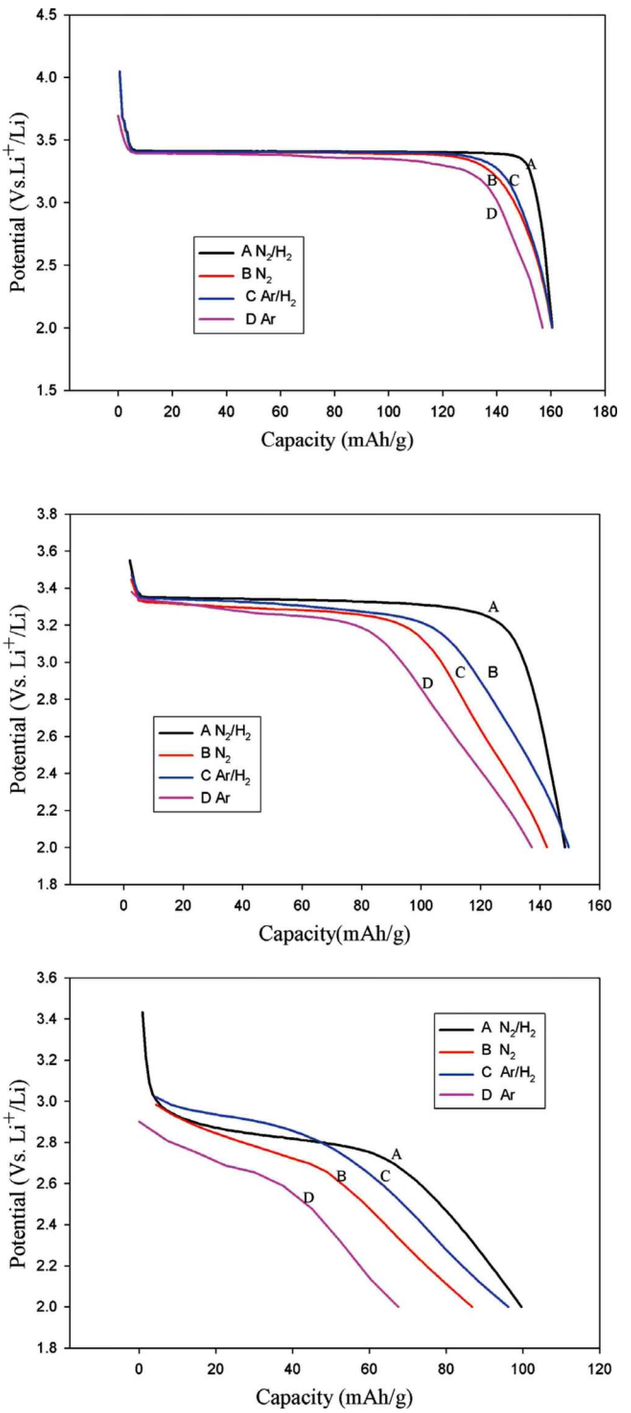

Figure 4. (Color online) Impact of gas treating atmosphere on capacity at (top) 0.1 C, (middle) C, and (bottom) 10 C rates.

and 15% vanadium materials formed in 5% hydrogen in argon. The Miller indexes are indicated in the 5% figure and the impurities in the 15% figure.

In order to see the crystal structure in detail, a full Rietveld refinement was carried out on three of the samples assuming the structural model of $LiFePO_4$. The lattice parameters determined are shown in Table I, and they show a slight but measurable decrease when vanadium is added. This is a clear indication of solid solution formation. The two earlier studies did not report any change in cell size, but an analysis by us of the impurity olivine phase formed by Padhi and Goodenough[21] while attempting to make the mixed Nasicon, $Li_3FeV(PO_4)_3$, in nitrogen also shows a smaller lattice with a volume of 288.2 $Å^3$, consistent with solid solution formation.

The Rietveld refinement fitting parameters showed an *R* factor of 10.6% assuming vanadium substitution on the iron site, and 7.6% assuming substitution on the phosphorus site for the 15% material. For the 5% material the *R* factor for substitution on the phosphorus

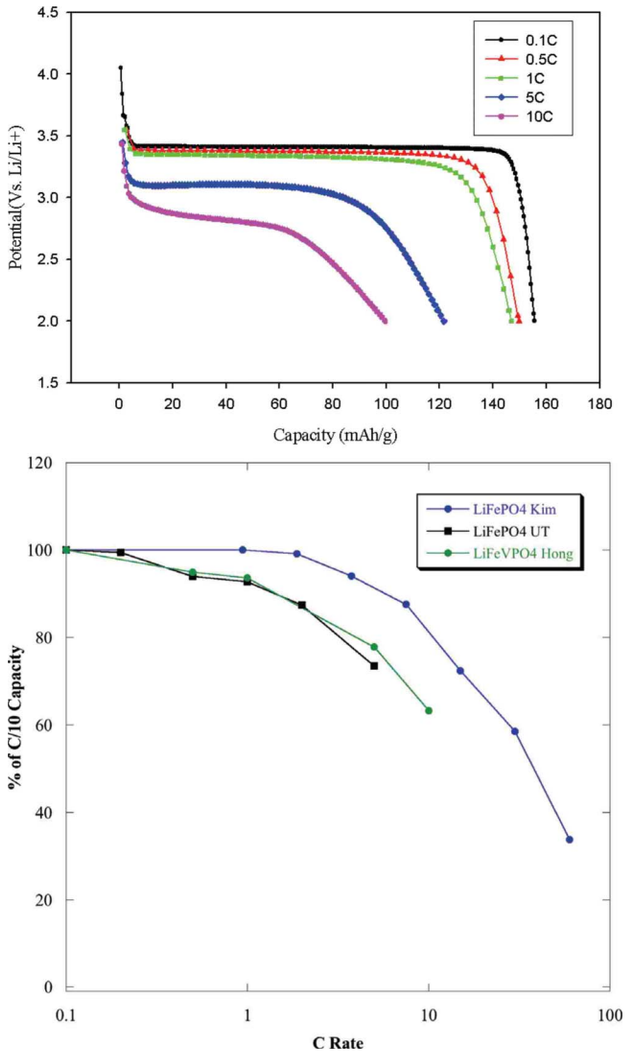

Figure 5. (Color online) (top) Discharge curves of $LiFeP_{0.95}V_{0.05}O_4$ at different C rates, and (bottom) its capacity compared with two high-rate solvothermal samples of $LiFePO_4$.[11,12]

site was 4.4%. Thus, although the vanadium was intended to substitute on the Fe sites in the olivine structure, the full Rietveld analysis clearly shows that the vanadium is located on the phosphorus site rather than on the iron site, giving materials of composition $LiFeP_{1-y}V_yO_4$.

For the $LiFeP_{0.95}V_{0.05}O_4$ material, an inspection of the diffraction pattern showed just a trace of the Fe_2P phase. However, for the $y = 0.15$ material, a multiphasic Rietveld indicated the presence of 90.4% $LiFeP_{0.85}V_{0.15}O_4$, 8% $Li_3(FeV)(PO_4)_3$, and 1.6% Fe_2P.

Morphology and microstructure.— The as-prepared materials show a microporous structure, as indicated in Fig. 2, for $LiFeP_{1-y}V_yO_4$ heat-treated in 5% hydrogen in argon. Each frame in the figure is about 10 × 10 μm. There is no well-defined, diamond-shaped morphology as found with hydrothermal samples,[3] but rather the particles appear as if generated from a gas-releasing foam. The "gas-holes" are as small as 100 nm. Each particle is constructed of smaller units that appear to be well-bonded together, leaving a microporous structure with pores ranging from a few micrometers to less than 100 nm. The vanadium-free compound appears to have the largest particle size and the highest degree of aggregation, which could explain its lower electrochemical capacity than the 5% vanadium material, as is discussed later. The crystallite size, within the particles, was determined from the linewidths using the Scherrer equation and was found to be around 50 nm. Thus, this synthesis method leads to a nanostructured but micrometer-sized material with a rather low external surface area. This should allow rapid reaction within each grain while minimizing extraneous surface reactivity and minimize the amount of surface that needs a conductive additive, such as carbon.

As Fig. 2 shows, there is not a great deal of difference between the samples with the different vanadium contents, suggesting that the microstructure is determined in the precursor stage prior to heating at 700°C. This emphasizes the importance of the initial stages in the formation of the olivine compounds to control the final morphology/microstructure. The heat-treating gas also did not have a major impact on the microstructure, suggesting again that it is in the initial formation during the precursor generation that the microstructure is formed. Delacourt et al.[14] similarly reported that the final firing step did not result in major changes in the olivine's morphology. The microstructure can be critical in determining the ultimate electrochemical performance of the $LiFePO_4$,[13] because the microstructure can decrease the lithium-ion diffusion distance by limiting particle size growth.

Electrochemical behavior.— The discharge characteristics of the $LiFeP_{1-y}V_yO_4$ materials, synthesized in the hydrogen-containing argon gas, are shown in Fig. 3. The vanadium content is found to have a dramatic effect on the capacity. At all discharge rates, the 5% vanadium sample outperforms all the other compositions, approaching 160 mAh/g at 0.1 C rate and exceeding 100 mAh/g at 10 C rate. The theoretical capacity of this material is about 160 mAh/g, as there is no evidence from the cycling curves that the vanadium is electrochemically active so only 95% of the lithium can be cycled. The pure $LiFePO_4$ loses more than 75% of its capacity as the rate is increased from C/10 to C. As the vanadium content is increased beyond 5%, the capacity drops off dramatically. This is partly due to the reduction in the amount of the redox active iron present, but possibly also due to possible resistive, either electronic or ionic, films on the surface of the active olivine material. The conductivity of these materials is discussed below.

As $LiFeP_{0.95}V_{0.05}O_4$ shows the best performance, it was selected for a study of the effect of heat-treatment atmosphere on the performance. The discharge curves are shown in Fig. 4 for three different rates, C/10, C, and 10 C. At the lowest rate there is no difference in total capacity, all achieving the theoretical value of 160 mAh/g. However, there is more polarization, and therefore energy loss, in the hydrogen-free argon material. This polarization becomes more marked at the C rate, with both of the hydrogen treated samples showing the best performance. As the rate is increased to 10 C, there

Table II. Comparison of characteristics of three high rate $LiFePO_4$ cathode materials.

Sample	Size (nm)	Carbon (wt %)	Binder (wt %)	$LiFePO_4$ (wt %)	Loading (mg/cm^2)	Reference
$P_{0.95}V_{0.05}$	50	6	6	88	4	This work
Fe	40	30	Included	70	2.8	11
Fe	25 × 100	20	5	75	10	12

Table III. Electronic and ionic conductivity of $LiFeP_{1-y}V_yO_4$.

y= Conductivity	0	0.05	0.075	0.10	0.15	0.20
Electronic (S/cm)	2×10^{-10}	3.2×10^{-6}	2×10^{-10}	3.5×10^{-10}	3.2×10^{-10}	3×10^{-10}
Ionic (S/cm)	3.2×10^{-6}	1.2×10^{-5}	2.3×10^{-6}	2.6×10^{-6}	8.6×10^{-6}	1×10^{-7}

is a marked dropoff in capacity with the materials synthesized in the presence of hydrogen, again showing the best performance with higher capacities and higher energy densities.

The rate capability of this material is comparable to some of the highest known for $LiFePO_4$. Figure 5a shows the discharge curves of the $LiFeP_{0.95}V_{0.05}O_4$ material for rates from C/10 to 10 C. Figure 5 (top) compares this material to two nanosized pure $LiFePO_4$ samples formed by a polyol/solvothermal reaction.[11,12] The vanadium compound has very comparable electrochemistry to the $LiFePO_4$ formed by a microwave/solvothermal process,[12] but the cathode contains less than 1/3 the amount of conductive diluent than the nanomaterial. It does not show as high a power capability as the nanosized $LiFePO_4$ formed solvothermally at 350°C,[11] but here again that material had much less active material in the cathode. The characteristics of all three materials are shown in Table II. Taking into account the weights of inactive material, this vanadium material has a higher capacity at all rates per total weight of cathode and much higher per unit volume of cathode. The rate capability is almost identical to that of $LiFe_{0.95}Mg_{0.05}PO_4$ made by the same procedure,[22,23] which strongly suggests that a low level of substitution on either site creates lattice disorder or defects, which reduces the energy to nucleate the two-phase region between $LiFePO_4$ and $FePO_4$.

Ionic and electronic conductivity.— Impedance spectroscopy was used to measure the ionic and electronic conductivity and interpreted as done for $LiFe_{0.95}Mg_{0.05}PO_4$.[22,23] The results, shown in Table III for the $LiFeP_{1-y}V_yO_4$ samples heat-treated in the 5% hydrogen in argon mixture, indicate a large increase in the electronic conductivity just for the 5% sample. This sample also exhibited the highest ionic conductivity. The heat-treatment atmosphere did not have a marked impact on either the ionic or electronic conductivity, with the former around 1.1–1.5 $\times 10^{-5}$ S/cm (except for the pure argon sample which was only 1.5×10^{-6} S/cm). The electronic conductivity also only varied from 1.0 to 3.2×10^{-6} S/cm, except again for the argon-treated sample, which was 1.2×10^{-7} S/cm. Thus, the vanadium is the critical player and its amount must be limited to around 5%.

GITT measurements.— The voltage profile of $LiFeP_{0.95}V_{0.05}O_4$ was measured by GITT. Although GITT is designed for studying the chemical diffusion coefficient in single-phase systems by following the voltage after a titration current pulse, it can still provide useful information in two-phase systems such as $LiFePO_4/FePO_4$. In this case the cell voltage will return to its initial state after a current pulse, but the speed at which this occurs can give us some comparative information about the electrode kinetics. Figure 6 shows the titration curves for three heat-treated samples of $LiFeP_{0.95}V_{0.05}O_4$. The current pulses in this case were from 5-12 $\mu A/cm^2$ for 2 h, and the voltage relaxation was followed for 3 h. It is clear that the polarization is much lower in the samples heat-treated in a hydrogen environment. In the case of the material treated in hydrogen-containing argon atmosphere, there is very little polarization except at the beginning and end of charge. This is to be expected as the few remaining vacant regions or lithium regions can be readily trapped by the neighboring region. When there are equal amounts of reacted and unreacted phase, then there is the highest probability of finding a reaction front. The sample treated in the hydrogen-containing nitrogen atmosphere shows slightly higher polarization and slower kinetics in returning to equilibrium. Finally, the sample treated in the

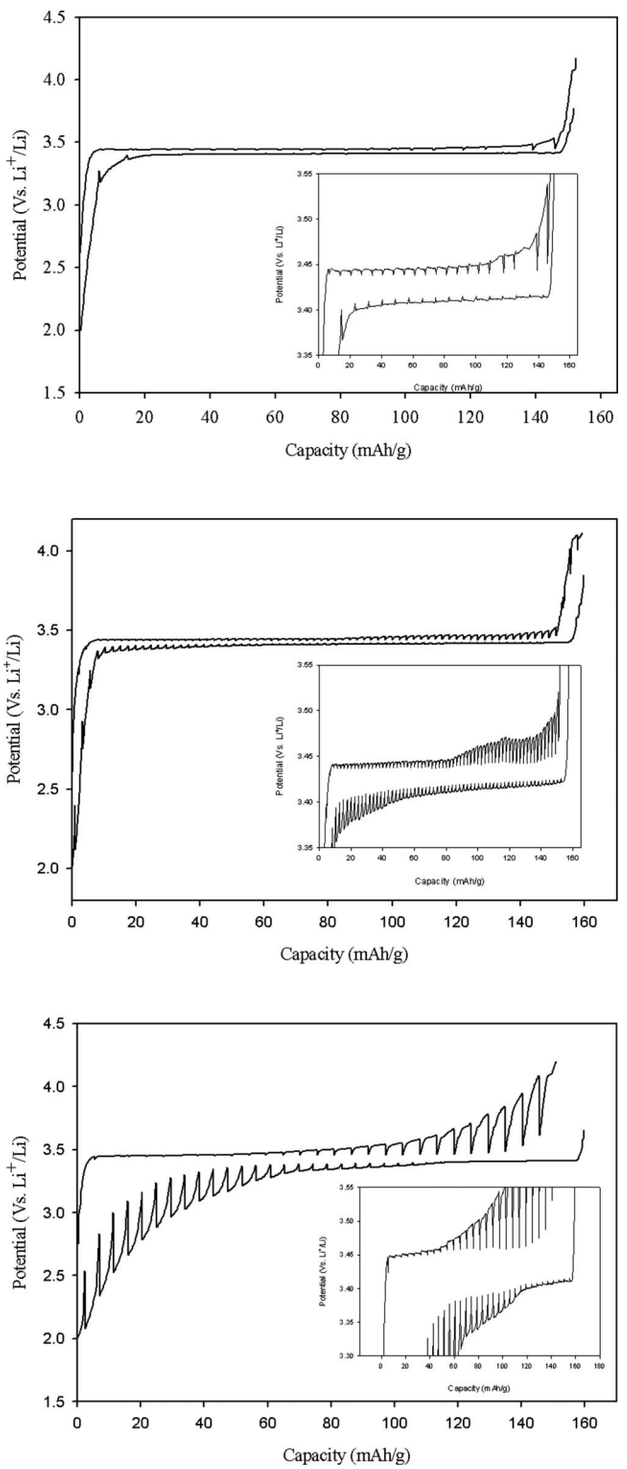

Figure 6. GITT for the V-doped $LiFePO_4$ heat-treated in (top) 5% H_2 in argon, (middle) 5% H_2 in nitrogen, and (bottom) pure argon.

inert argon atmosphere shows a much higher overpotential and slower kinetics for all stages of charge and discharge. These results clearly show the advantages of using a reducing atmosphere in the synthesis of these vanadium-containing olivine compounds.

Conclusions

Vanadium ions can be incorporated into the iron-containing olivine structure of $LiFePO_4$, as evidenced by the change in lattice parameters. The oxidation state, amount, and exact location in the lattice is not known and will need to be determined when single crystals are available. A small amount of vanadium, around 5%, enhances the rate capability of the $LiFePO_4$ olivine cathode without significantly impacting its capacity. Higher levels of vanadium reduce the power capability below that of the pure $LiFePO_4$. The 5% material had the highest electronic and ionic conductivities, and they were of comparable magnitude. The kinetics of the reaction were highest when a reducing atmosphere was used in the synthesis of the $LiFeP_{0.95}V_{0.05}O_4$ material. This vanadium material has power capabilities comparable to the highest obtained in nanosized $LiFePO_4$ but while only using a 6% conductive carbon loading. Its presence likely creates lattice disorder and defects which reduces the energy needed to nucleate the two-phase region $LiFePO_4$ $FePO_4$ region.

Acknowledgment

We thank the United States Department of Energy, Office of FreedomCar and Advance Vehicle Technologies, for support of the work at Binghamton, through the BATT program at Lawrence Berkeley National Laboratory.

Binghamton University assisted in meeting the publication costs of this article.

References

1. A. K. Padhi, K. S. Nanjundaswamy, C. Masquelier, and J. B. Goodenough, *J. Electrochem. Soc.*, **144**, 2581 (1997).
2. M. S. Whittingham, Y. Song, S. Lutta, P. Y. Zavalij, and N. A. Chernova, *J. Mater. Chem.*, **15**, 3362 (2005).
3. J. Chen, M. J. Vacchio, S. Wang, N. Chernova, P. Y. Zavalij, and M. S. Whittingham, *Solid State Ionics*, **178**, 1676 (2008).
4. O. V. Yakubovich, V. V. Bairakov, and M. A. Simonov, *Dokl. Akad. Nauk SSSR*, **307**, 1119 (1989).
5. S. Chung, J. T. Bloking, and Y. Chiang, *Nature Mater.*, **1**, 123 (2002).
6. P. S. Herle, B. Ellis, N. Coombs, and L. F. Nazar, *Nature Mater.*, **3**, 147 (2004).
7. M. S. Islam, D. J. Driscoll, C. A. J. Fisher, and P. R. Slater, *Chem. Mater.*, **17**, 5085 (2006).
8. N. Ravet, J. B. Goodenough, S. Besner, M. Simoneau, P. Hovington, and M. Armand, Abstract 127, The Electrochemical Society and The Electrochemical Society of Japan Meeting Abstracts, Vol. 99-2, Honolulu, HI, Oct 17–22, 1999.
9. H. Huang, S. C. Yin, and L. F. Nazar, *Electrochem. Solid-State Lett.*, **4**, A170 (2001).
10. G. Chen, X. Song, and T. J. Richardson, *Electrochem. Solid-State Lett.*, **9**, A295 (2006).
11. D.-H. Kim and J. Kim, *Electrochem. Solid-State Lett.*, **9**, A439 (2006).
12. A. V. Murugan, T. Muraliganth, and A. Manthiram, *Electrochem. Commun.*, **10**, 903 (2008).
13. R. Dominko, J. M. Goupil, M. Bele, M. Gaberscek, M. Remskar, D. Hanzel, and J. Jamnik, *J. Electrochem. Soc.*, **152**, A858 (2005).
14. C. Delacourt, P. Poizot, S. Levasseur, and C. Maquelier, *Electrochem. Solid-State Lett.*, **9**, A352 (2006).
15. N. Meethong, H.-Y. S. Huang, W. C. Carter, and Y.-M. Chiang, *Electrochem. Solid-State Lett.*, **10**, A134 (2007).
16. M. S. Whittingham, *Science*, **192**, 1126 (1976).
17. Z. Chen and J. R. Dahn, *J. Electrochem. Soc.*, **149**, A1184 (2002).
18. Y. Song, P. Y. Zavalij, and M. S. Whittingham, *J. Electrochem. Soc.*, **152**, A721 (2005).
19. Y. Wen, L. Zeng, Z. Tong, L. Nong, and W. Wei, *J. Alloys Compd.*, **416**, 206 (2005).
20. M.-R. Yang, W.-H. Ke, and S.-H. Wu, *J. Power Sources*, **165**, 646 (2007).
21. A. K. Padhi and J. B. Goodenough, Unpublished work, 1994.
22. C. S. Wang and J. Hong, *Electrochem. Solid-State Lett.*, **10**, A65 (2007).
23. J. Hong, C. S. Wang, and U. Kasavajjula, *J. Power Sources*, **162**, 1289 (2006).